# Raman Lidar Measurements of Water Vapor and Aerosols During the Atmospheric Radiation Measurement (ARM) Remote Cloud Sensing (RCS) Intensive Observation Period (IOP)

*S.H. Melfi, D. O'C. Starr, and D. Whiteman*
*NASA Goddard Space Flight Center*
*Greenbelt, Maryland*

*R. Ellingson*
*University of Maryland*
*College Park, Maryland*

*R. A. Ferrare and K. D. Evans*
*Hughes STX*
*Lanham, Maryland*

The first Atmospheric Radiation Measurement (ARM) Remote Cloud Study (RCS) Intensive Operations Period (IOP) was held during April 1994 at the Southern Great Plains (SGP) Cloud and Radiation Testbed (CART) site near Lamont, Oklahoma. This experiment was conducted to evaluate and calibrate state-of-the-art, ground-based remote sensing instruments and to use the data acquired by these instruments to validate retrieval algorithms developed under the ARM program. These activities are part of an overall plan to assess general circulation model (GCM) parameterization research. Since radiation processes are one of the key areas included in this parameterization research, measurements of water vapor and aerosols are required because of the important roles these atmospheric constituents play in radiative transfer.

The National Aeronautics and Space Administration (NASA)/Goddard Space Flight Center (GSFC) Scanning Raman Lidar (SRL) acquired more than 123 hours of water vapor and aerosol profile data during 15 nights of operations. The lidar acquired vertical profiles as well as nearly horizontal profiles directed near an instrumented 60-m tower. We also deployed a multi-band automatic sun and sky scanning radiometer at this site which acquired aerosol and water vapor data throughout this experiment. Aerosol optical thickness, phase function, size distribution, and integrated water vapor were derived from a combination of sun and sky brightness measurements measured by this instrument. We used measurements from both instruments to assess the water vapor and aerosol measurements made by other instruments during the IOP, studied the structure and dynamics of a cold front which passed over the site on the night of April 15, 1994, and studied the aerosol optical and physical properties of aerosols.

## Instruments

The GSFC Scanning Raman lidar uses an XeF excimer laser to transmit light at 351 nm. Light backscattered by molecules and aerosols at the laser wavelength is detected as well as Raman scattered light from water vapor (403 nm), nitrogen (382 nm), and oxygen (371 nm) molecules. The signals are gathered by a 76-cm-diameter telescope, detected by photomultiplier tubes, and recorded using photon counting. A steerable elliptical flat provides full 180 degree horizon to horizon scan capability within a single scan plane. The scan capability was used to increase the vertical resolution of the data as well as to facilitate comparisons with tower-based instruments. Water vapor mixing ratio was derived from the ratio of water vapor to nitrogen Raman signals; relative humidity was computed from the water vapor mixing ratio and radiosonde pressure and temperature measurements. Aerosol scattering ratio profiles were derived from the Raman nitrogen return signal and the signal detected at the laser wavelength; the aerosol volume backscattering cross section was then computed from the scattering ratio and from the molecular volume backscatter cross section calculated from coincident CART radiosonde density data. The aerosol extinction cross section is computed from the derivative of the Raman nitrogen return signal with respect to range. Details of these procedures are discussed by Ferrare et al. (1992, 1993) and Whiteman et al. (1992).

The Cimel Electronique 318A radiometer, which we deployed at the CART site, is a compact, weather-resistant system which operates independently of commercial electrical and communication systems. Two detectors permit the measurement of direct solar, aureole, and sky radiance.

During the RCS IOP, the instrument used six interference filters to acquire aerosol measurements at the following wavelengths: 339, 380, 441, 672, 873, and 1022 nm. Two additional filters at wavelengths near the 940-nm water vapor absorption band were used to estimate total precipitable water vapor. The sensor head is positioned by two microprocessor controlled motors to automatically acquire solar radiance observations throughout each day; aerosol optical thicknesses are derived from these observations. Additional sky radiance measurements made at the solar zenith angle for specified azimuth angles (almucantar) are used to derive the aerosol size distribution using inversion algorithms (Kaufman et al. 1994).

## Measurements

The SRL acquired vertical profiles as well as data at scan angles 5 and 10 degrees above the horizon on nine nights during the IOP. Figure 1 shows examples of images

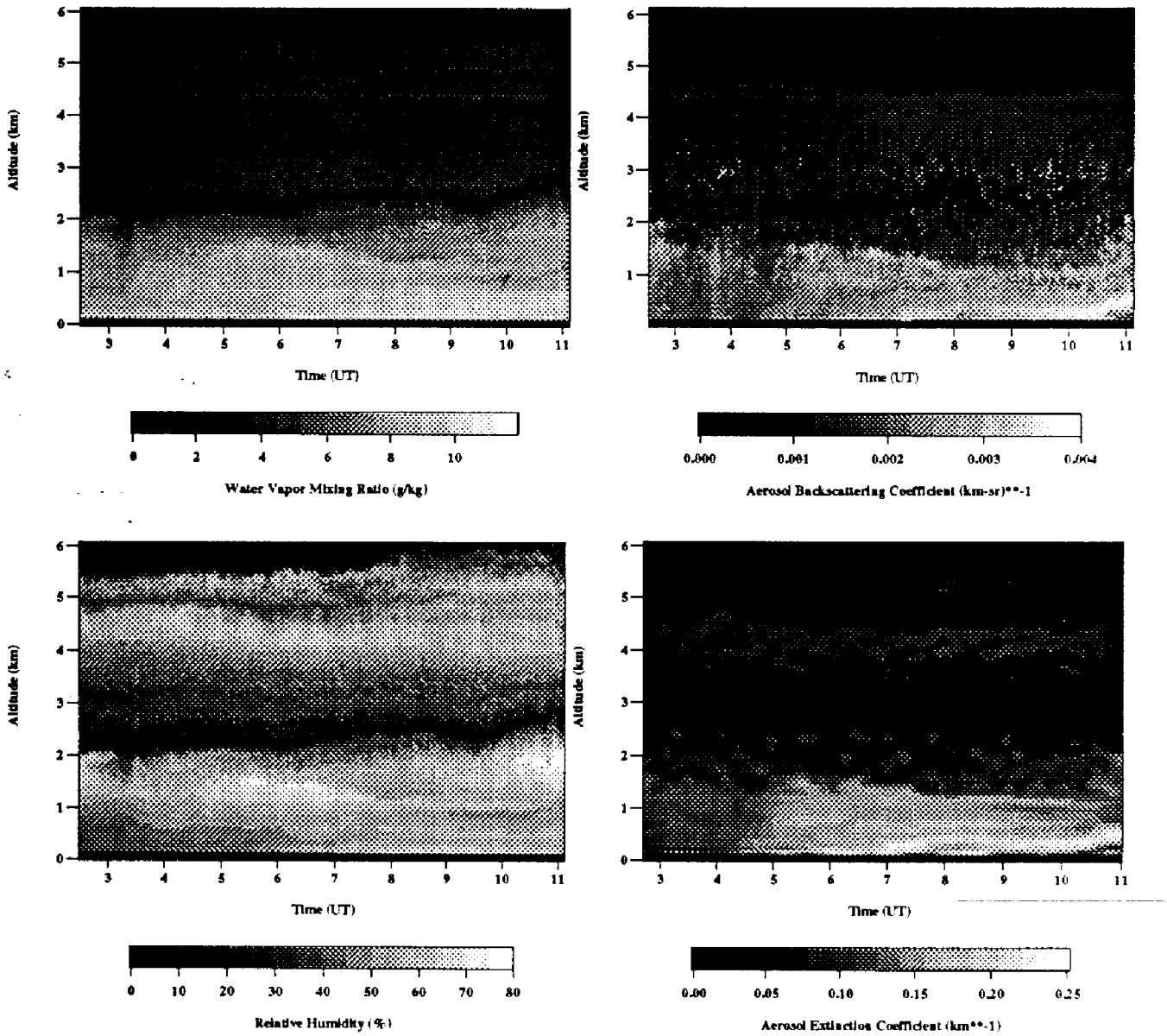


**Figure 1**. Water vapor mixing ratio (top left), relative humidity (bottom left), aerosol backscatter (top right), and aerosol extinction (bottom right) coefficients measured by Scanning Raman Lidar on April 21, 1994.

displaying water vapor mixing ratio, relative humidity, aerosol backscatter, and extinction coefficients acquired on April 21, 1994. These images, which were constructed using several hundred water vapor and aerosol profiles acquired simultaneously on the night of April 21, 1994, show water vapor and aerosols mainly concentrated in the residual layer below about 1.5 km. A dry, clean layer separates this residual layer from an elevated layer of water vapor and aerosols.

Figure 2 shows excellent agreement between the relative humidity profiles derived from SRL data acquired on this night and the humidity profiles measured by coincident Vaisala radiosondes launched at the CART site. On this same night, the University of North Dakota Citation aircraft flew above the CART site and acquired both water vapor and aerosol measurements. Both the lidar measurements of aerosol backscattering and extinction as well as the aerosol number density profiles measured by an optical particle counter on the aircraft showed increasing amounts of aerosols in the residual layer through this night.

The lidar and sun photometer measurements show changes in both water vapor and aerosols which occurred during this experiment. Figure 3 shows precipitable water vapor and aerosol optical thickness $\tau_a$ measured by the lidar at night as well as by the sun photometer during the day. The precipitable water and aerosol optical thickness values were generally highly correlated during the IOP; increases in both the precipitable water vapor and aerosol optical thickness between April 19-25, 1994, were indicative of changes in air mass characteristics over the CART site at this time.

The simultaneous increase in the wavelength dependence of aerosol optical thickness measured by the sun photometer during this period was most likely caused by an increase in the number of small particles associated with a change in the air mass as shown by air trajectory analyses. The lidar measurements of aerosol backscattering and extinction also indicated changes in aerosol properties during the period.

In addition to studying changes in aerosol optical properties, the lidar measurements have been used to study atmospheric dynamics. The vertical structure and temporal evolution of a cold front was dramatically revealed by the lidar water vapor and aerosol data acquired on the night of April 15, 1994. Figure 4 shows water vapor mixing ratio and aerosol scattering ratio measured by the lidar. The lidar data show the increase of moisture ahead of the front, oscillations along the sloping frontal surface, and the decrease in moisture and aerosols after frontal passage. Figure 3 shows an increase in precipitable water and aerosol optical thickness prior to the passage of the cold front. Starr et al. (1995) have used these lidar data along with surface mesonet data to study the structure and dynamics of this cold front.

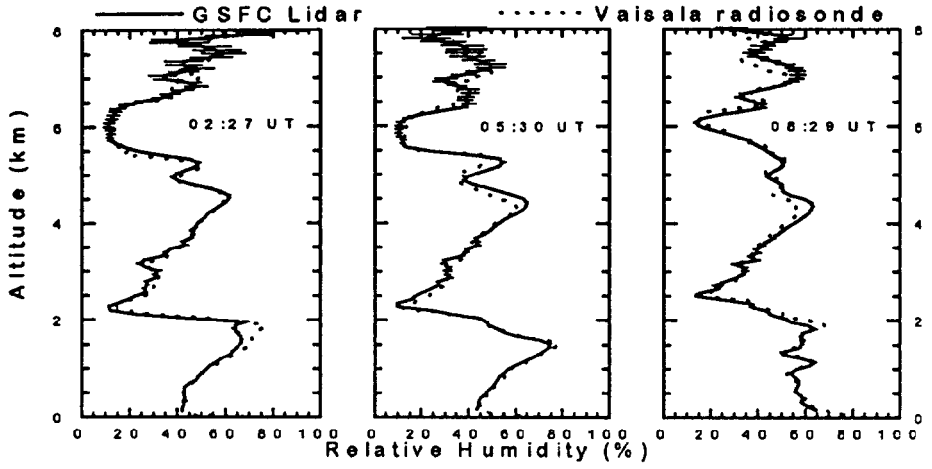


**Figure 2**. Relative humidity profiles derived from one-minute lidar water vapor profiles at 02:27 UT, 05:30 UT, and 08:29 UT on April 21, 1994. Profiles measured by coincident Vaisala radiosondes are also shown.

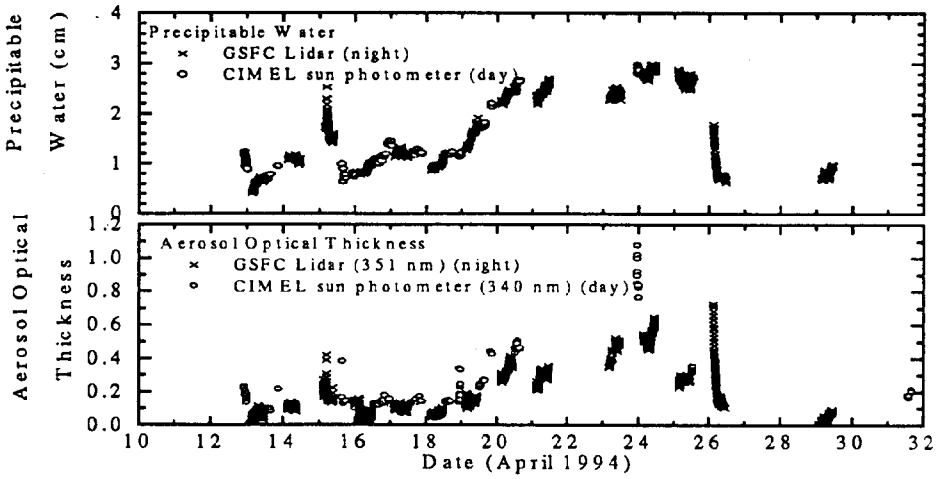


**Figure 3**. Precipitable water vapor (top) and aerosol optical thickness $\tau_a$ (bottom) measured by the Raman lidar and sun photometer.

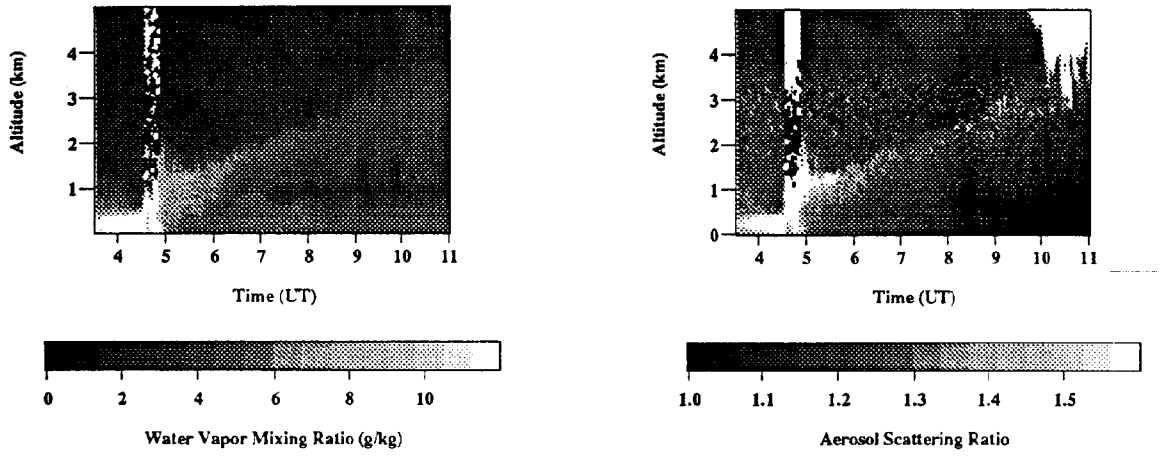


**Figure 4**. Water vapor mixing ratio (left) and aerosol scattering ratio (right) measured by the Scanning Raman Lidar showing the passage of a cold front over the CART site on the night of April 15, 1994.

## References

Ferrare, R. A., S. H. Melfi, D. N. Whiteman, and K. D. Evans. 1992. Raman lidar measurements of Pinatubo aerosols over southeastern Kansas during November-December 1991, *Geophys. Res. Lett.*, **19**(15), 1599-1602.

Ferrare, R. A., S. H. Melfi, D. N. Whiteman, and K. D. Evans. 1993. Coincident measurements of atmospheric aerosol properties and water vapor by a scanning raman lidar. In *Optical Remote Sensing of the Atmosphere Technical Digest*, Vol. 5, 11-14. Optical Society of America, Washington, D.C.

Kaufman, Y. J., A. Gitelson, A. Karnieli, E. Ganor, R. S. Fraser, T. Nakajima, S. Mattoo, and B. N. Holben. 1994. Size distribution and scattering phase function of aerosol particles retrieved from sky brightness measurements, *J. Geophys. Res.*, **99**(D5), 10341-10356.

Starr, D. O'C., S. H. Melfi, A. R. Lare, R. A. Ferrare, D. Whiteman, K. D. Evans, B. Demoz, G. Mace, K. Sassen, and S. E. Bisson. 1995. Observations of a cold front with strong vertical undulations during the ARM RCS IOP, *Proceedings of the Fifth ARM Science Team Meeting*, this issue.

Whiteman, D. N., S. H. Melfi, and R. A. Ferrare. 1992. Raman lidar system for the measurement of water vapor and aerosols in the earth's atmosphere, *Appl. Opt.*, **31**(16), 3068-3082.